

Chemical and optical properties of the titanium dioxide produced from combustion of titanium microparticles in air

V.S. Zakharenko,¹ V.N. Parmon,¹ and S.A. Khromova²

¹*G.K. Boreskov Institute of Catalysis,
Siberian Branch of the Russian Academy of Sciences, Novosibirsk*
²*Novosibirsk State University*

Received February 21, 2007

It is shown that the solid titanium dioxide aerosol, obtained from combustion in air of a pyrotechnic mixture containing titanium microparticles, has optic, chemical, and photocatalytic properties similar to those of titanium dioxide produced in other ways. An aerosol cloud produced from such titanium dioxide immediately in the place of abrupt emission of pollution favors purification of the gas-phase atmosphere nearby the pollution source.

Introduction

Earth's atmosphere is able to self-purify of some detrimental compounds due to oxidation processes and destruction of these compounds on the surface of aerosol particles under the action of solar radiation. In particular, these processes can eliminate many ozone-depleting compounds and greenhouse gases from the atmosphere. However, in cases of technogenic catastrophes and large-scale terrorist attacks, accompanied by instantaneous emission of pollutants, the purification of the atmosphere by means of photostimulated processes on aerosols on their natural level can be ineffective.

One of the approaches to the problem of air purification from local pollutions can be the dispersion in the emission zone of metal-oxides-containing artificial aerosol, active in photocatalytic and/or photosorption processes. Such photoactive artificial aerosols can be obtained, e.g., from combustion in air of a pyrotechnic mixture with high concentration of aluminium,¹ titanium,² magnesium,³ etc.

Indeed, it is well known, that magnesium oxide is an effective photosorbent of halogen organic compounds⁴ while titanium dioxide is an active and stable photocatalyst of mineralization (deep air oxidation) of many organic and inorganic compounds.⁵

In this work, the chemical properties of titanium dioxide, produced from combustion of a pyrotechnic mixture in air, and changes of these properties under the action of solar radiation are studied.

Experimental technique

To obtain titanium dioxide, a pyrotechnic mixture was prepared of ammonium perchlorate, hydroxyl-terminated polybutadiene (HTPB), and particles of metallic titanium of micron size (fraction from 60 to 90 μm). After mixture combustion in air in a glass container of 20 l in volume, the produced powder of titanium dioxide was gathered from the

container's walls. The water suspension of the powder was applied on the internal wall of a quartz photoreactor. After room-temperature drying in air, the reactor was soldered to a high-vacuum experimental setup. The detailed description of the experiment is given in Ref. 6.

The titanium dioxide powder, produced from the combustion of the pyrotechnic mixture in air (the production technique is described in Refs. 7 and 8), has a specific area of 6 m^2/g . After powder heating at 625 K during 30 min in air, its specific area decreases to 4 m^2/g . The specific area was measured in the Adsorption Laboratory of the Institute of Catalysis SB RAS. According to the data of X-ray crystallography, the presence of TiO_2 in crystal modifications (rutile and anatase) is observed in the titanium dioxide powder, part of which was used in our experiment.

In this experiment were used freon 134a ($\text{CF}_3\text{CH}_2\text{F}$) given by RSC "Applied chemistry" (St. Petersburg) and freon 22 (CHF_2Cl) produced by Ural PA "Galogen." Before the use, the compounds were additionally purified by freezing at the temperature of liquid nitrogen.

Amount and content of gases in the reaction volume were determined with a Pirani manometer and mass-spectrometer, assembled on the base of a partial-pressure gage APDM-1 when gas flowing up through a leak valve (see also Ref. 6).

If required, the composition of gas mixture in the reaction volume was controlled (before, during, and after dark and photoadsorption of gases) by means of condensation analysis. Peak values and peaking time on the curve of time dependence of pressure in the measurement volume were registered during defrosting of nitrogen-temperature condensed gases when temperature rising from liquid nitrogen to room one. The condensation analysis was accompanied by the mass-spectrometric analysis to identify the defrosting peaks; in this case, the mass-spectrometer operated in the scanning several masses mode or adjusting to the expected-mass mode.

For UV-irradiation of TiO_2 surface, the OSL-1 light for fluorescence microscopes with Hg-lamp DRSh-250, heat water, and UVC filters was used. Total irradiance on the front wall of the photoreactor, measured with a RTN-20C thermopile, was about 1 mW/cm^2 for the UVC filter.

The quantum efficiency of the photodesorption and photoabsorption was defined as the ratio of the number of photodesorbed and photoabsorbed molecules, respectively, to the number of quanta passed from the lighter through the front reactor's wall. To separate monochromatic radiation, interference filters were used.

Diffuse reflection spectra were recorded in air with the SPECORD M40 spectrophotometer (Germany); the powder of magnesium oxide was used as the reflection standard.

Results and discussion

1. Optical properties of titanium dioxide powder samples

Absorptivity of the surface of disperse titanium dioxide, produced from combustion of titanium microparticles in air, was under study. A part of titanium dioxide powder has been holding in air for long time, another part was heat-treated at the temperature of 625 K in air during 30 min. Experiments with samples, being in long-term contact with air, model the use of titanium dioxide aerosols obtained with the above technique, in the processes resulting in air purification during technogenic catastrophes of different nature.

Titanium dioxide has three stable crystal modifications occurring in nature in the form of rutile, anatase, and brookite.⁹ Stoichiometric samples of titanium dioxide of all the above crystal modifications are white powders. Quantum absorption by such powders is minimal in the range of quantum energies less than band gap of rutile ($E_g = 3.05 \text{ eV}$) (Figs. 1*a, b*). This absorption corresponds to the band of extrinsic absorption for monocrystals or surface absorption for finely dispersed powders.

According to these data, if powder samples of titanium dioxide consist of the mixture of rutile and anatase, then a knee on the absorption edge curve is observed (Fig. 1*a*, curves 1 and 2 and Fig. 1*b*, curve 1). This knee is absent for anatase (Fig. 1*b*, curve 2) or rutile (Fig. 1*c*, curve 1) modifications. Titanium dioxide produced by "Degussa" company contains rutile and anatase along with amorphous phase.¹⁰ The powder anatase absorption edge is 0.1–0.2 eV shifted to the shortwave side relative to the powder rutile absorption edge (3.0 and 2.8–2.9 eV, respectively).

Stoichiometry of titanium dioxide can be violated due to partial reduction of Ti^{4+} to Ti^{3+} and formation of lattice oxygen vacancies, e.g., while oxide producing. In this case, powder TiO_2 samples

are colored and absorption in the range of oxide surface absorption is appeared.

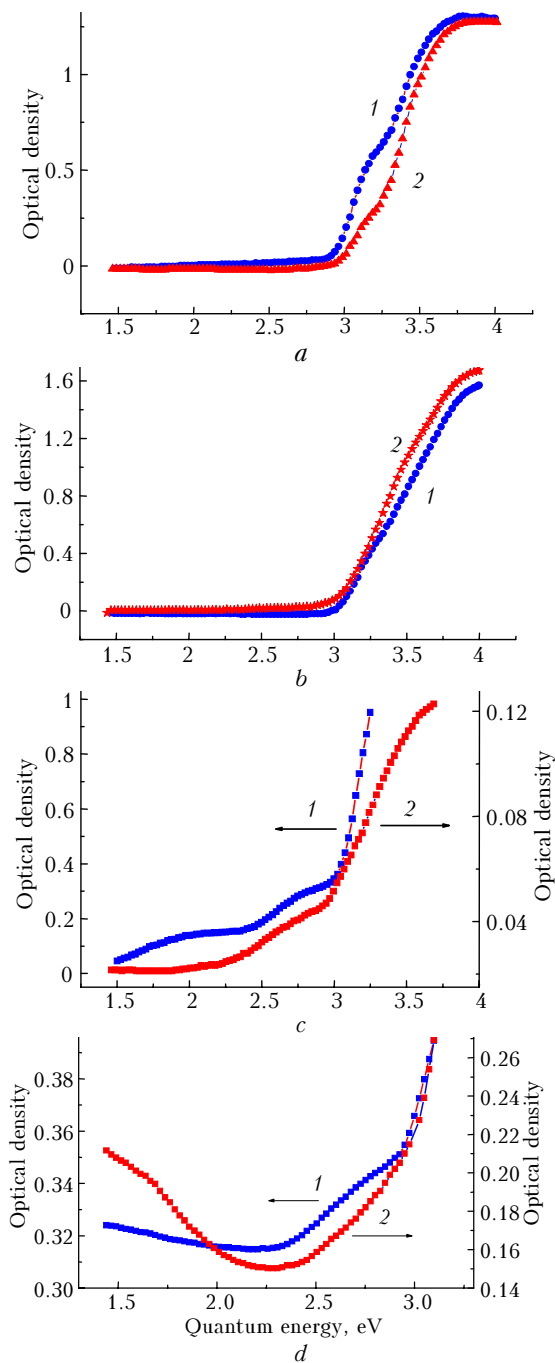


Fig. 1. Spectra of diffuse reflection optical density (SDF) of titanium dioxide samples measured relative to MgO . *a*: plasmatron producing, specific area $3 \text{ m}^2/\text{g}$, produced in Russia (1); anatase warmed up at 1270 K, $8 \text{ m}^2/\text{g}$, Russia (2); *b*: plasmatron producing, $50 \text{ m}^2/\text{g}$, "Degussa" company (1); plasmatron producing, $100 \text{ m}^2/\text{g}$, France (2); *c*: greenish rutile, Institute of Catalysis (1); titanium dioxide used in the reactor (mixture of rutile and anatase) (2); *d*: after the reactor titanium dioxide warming up at 620 K during 30 min (1); titanium dioxide sampled from gas phase immediately after pyrotechnic mixture combusting with the use of a vacuum impactor (2).

The diffuse reflection spectrum of TiO_2 powder, green due to nonstoichiometric composition, obtained at the Institute of Catalysis SB RAS, is shown in Fig. 1*b* (curve 1). According to the data of X-ray structure analysis, this powder contains titanium dioxide in rutile crystal modification. Greenish titanium dioxide powder, produced from combustion of a peroxide mixture, contains rutile modification of TiO_2 in mixture with anatase one. In this case, the EPR method confirms disrupted stoichiometry of titanium dioxide powder, used in photosorption experiments, by signals from Ti^{3+} cations.

The diffuse reflection spectrum (Fig. 1*c*, curve 2) is also an evidence of TiO_2 stoichiometry disruption. Note that titanium dioxide powder, used for recording the absorption spectra, was not after-treated; similar titanium dioxide sample was used in the application on the photoreactor's walls. The optical density spectrum of diffuse reflection for titanium dioxide warmed up in air at the temperature of 620 K during 30 min is shown in Fig. 1*d* (curve 1). Here (curve 2) the spectrum of titanium dioxide, sampled from gas phase with the use of a vacuum impactor (vacuum gas sampler of SP line worked out at the Institute of Chemical Kinetics and Combustion SB RAS) immediately after pyrotechnic mixture combusting is also shown.

Thus, optical absorptivity of powder samples of titanium dioxide, produced from combustion of a pyrotechnic mixture containing titanium microparticles in air, depends on the producing technique and further treatment of the samples in the range up to the TiO_2 self-absorption edge (corresponds to the part of spectrum of solar tropospheric radiation).

2. Chemical and photosorption properties of titanium dioxide produced from combustion of titanium microparticles in air

When pumping out the photoreactor with applied TiO_2 at the room temperature, mainly water and carbonic acid gas are desorbed from the titanium dioxide surface. In the course of the described experiments, water vapors are always present in the photoreactor volume; when uniting the reactor and measurement volumes, water vapors are caught in the reactor volume by a trap with the cooling mixture (ethyl alcohol cooled to a temperature of 173 K). Long-lasting (during 1 hour) pumping out of the reactor volume in the high-vacuum setup through the trap with cooling mixture results in partial desorption of carbonic acid gas, adsorbed on the titanium dioxide surface, and covering the quasi-equilibrium surface with carbon dioxide. Kinetics of dark stabilization of CO_2 equilibrium pressure is given in Fig. 2, curve 1.

This kinetics is represented as the reduction of the number of CO_2 molecules adsorbed on the titanium dioxide surface due to desorption; the observed kinetics corresponds to the first-order reaction with the time constant $\tau_1 \approx 6$ min.

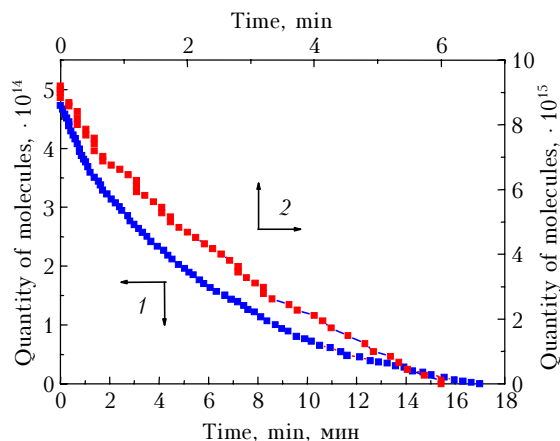


Fig. 2. Kinetics of CO_2 desorption from the TiO_2 surface: curve 1 is the dark quantity reduction of CO_2 molecules (dark desorption) on the TiO_2 surface; 2 is the CO_2 molecules number reduction (in addition to dark one) when TiO_2 surface illuminating through the UVC filter (photodesorption).

Desorption experiments with titanium dioxide produced from combustion in air of a pyrotechnic mixture, containing titanium microparticles, do not reveal any gases in noticeable amounts other than CO_2 and H_2O , evolved in the dark at the room temperature from the titanium dioxide surface.

Illumination of samples in the visible range results in additional CO_2 desorption (Fig. 2, curve 2). Kinetics of this desorption is similar to the kinetics of dark CO_2 desorption and is characterized by the time constant $\tau_2 \approx 5$ min, but the amount of photodesorbed carbon dioxide in this case is 20 times higher than in the dark. The photodesorption kinetics is shown in Fig. 2 as the number reduction of CO_2 molecules adsorbed on the TiO_2 surface.

Figure 3 presents mass-spectrometric data on intensity changes in peak of the 44th mass (basic peak of carbon dioxide in mass-spectrum) when TiO_2 illuminating through the 436 and 308 nm interference filters. The kinetics of CO_2 photodesorption in case of 436 nm filter (region of TiO_2 extrinsic surface absorption, see Fig. 1*c*) differs from those in case of 308 nm filter (region of TiO_2 self-absorption, see Fig. 1*c*) in the faster reduction of the rate of the dioxide carbon escape. In the first case, the kinetics better agrees with the kinetics of the first-order reaction like in the case of illuminating through the UVC filter (Fig. 2, curve 2). In the second case, the kinetics is described by a linear equation.

Measurements of spectral dependences of quantum efficiency of CO_2 photodesorption have shown the maximum of photodesorption quantum efficiency in the range of titanium dioxide self-absorption (Fig. 4, curves 1 and 2).

For comparison, the spectrum of diffuse reflection of titanium dioxide powder, used in this work, is also shown (curve 3). Prolongation of radiation effect on the TiO_2 surface up to several hours results in the decrease of quantum efficiency of carbon dioxide photodesorption.

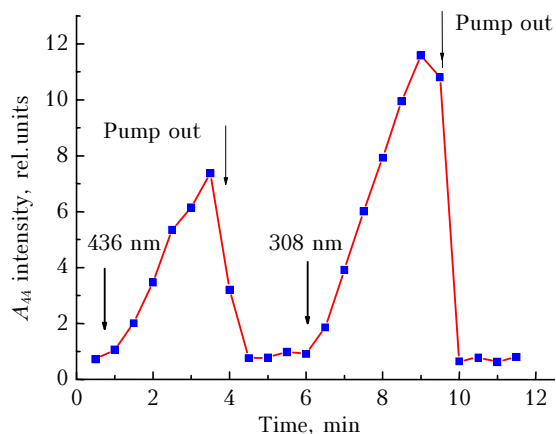


Fig. 3. Kinetics of CO_2 photodesorption from the TiO_2 surface when illuminating with quanta of about 436 and 308 nm wavelengths (mass-spectrometric data).

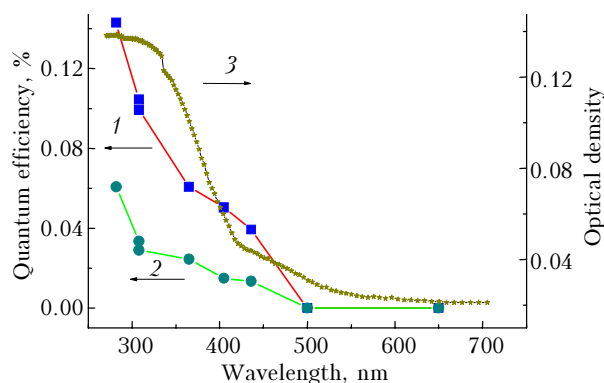


Fig. 4. Spectral dependences of quantum efficiency for titanium dioxide produced from combustion of titanium particles in air: CO_2 photodesorption at first illumination of a TiO_2 sample (1); CO_2 photodesorption after long-term illumination of the titanium dioxide surface through the UVC filter (2); SDF of titanium dioxide powder used in the reactor (3).

Within the TiO_2 self-absorption band (including those for 308 nm filter) the CO_2 photodesorption is probably associated with deep photocatalytic air oxidation of the adsorbed carbon-containing compounds.¹¹ Within the surface absorption band dominant are the processes associated with electron transport from the oxide valence band to the surface and discharging the surface compounds (for example, CO_3^- , CO_2^-) with electron transport to the conduction band. It can be supposed, that CO_2 photodesorption in the first case occurs while discharging surface carbonate and carboxylated groups¹² by a mobile hole of the valence band. In the second case, the CO_2 desorption is associated with the direct discharging of these compounds. The efficiency of absorption with electron-hole pairs formation is essentially higher than those in the surface absorption band (see Fig. 1c, curve 2). The photodesorption quantum efficiency in the titanium dioxide self-absorption band is also essentially higher than in the surface absorption band (see Fig. 4).

Photoadsorption of freon 22 (CHF_2Cl) and freon 134a ($\text{CF}_3\text{CH}_2\text{F}$) was not observed on the titanium dioxide, produced in the ambient air conditions and held in air for a long time under the effect of “full” radiation of Hg-lamp DRSh-250 or when illuminating through the UVC filter. Photoadsorption of these freons is also unobservable in the presence of dry air. According to reference data, photocatalytic oxidation of methane is unobservable on TiO_2 [Refs. 13, 14] But methane and hydrogen photoadsorption were observed on the titanium dioxide modification routine after its high-temperature oxygen-vacuum warming up.^{15–17} Photosorption of methane (freon 22) and ethane (freon 134a) modifications is registered and effective on MgO and CaCO_3 , long-term air exposed.^{4,18} At the same time, photocatalytic oxidation of carbon oxide¹¹ is effective on the titanium dioxide surface, as well as some other gas-phase reactions, e.g. photocatalytic oxidation of alkanes C_{2+} [Refs. 13, 14, and 19] and aromatic hydrocarbons,²⁰ photocatalytic destruction of chlorinated ethylene derivatives,^{21,22} etc.

We succeeded to observe oxygen photoadsorption from air, dried by passing through a nitrogen-cooled trap, on the TiO_2 surface. Photodesorption of carbon dioxide proceeds simultaneously with oxygen photoadsorption. The initial rate of oxygen photoadsorption exceeds the initial rate of CO_2 photodesorption. Pressure decrease (photoadsorption) is observed when registering total pressure with a Pirani manometer.

The kinetics of pressure decrease in the reaction volume when illuminating the titanium dioxide surface through the UVC filter is shown in Fig. 5, curve 1 (manometric data). Curve 2 here shows the kinetics of oxygen amount reduction (oxygen photoadsorption) by height variation of the 32nd mass peak in the mass-spectrum (mass-spectrometric data); the kinetic is described by a first-order equation with $\tau_3 \approx 3$ min. In this case, the oxygen from the reaction volume is fully photoadsorbed. The amount of photoadsorbed oxygen even at first illumination is five times as much as the amount of photodesorbed CO_2 . The kinetics of carbon dioxide photodesorption, in the presence of gas-phase oxygen, is characterized by significantly larger time constant ($\tau_4 \approx 10$ min, Fig. 5, curve 3) as compared with the time constants for dark desorption (τ_1) and CO_2 photodesorption (τ_2).

Measurements of spectral dependences of the quantum efficiency of oxygen photoadsorption from dry air has shown more efficient running of the photoabsorption in the range of titanium dioxide self-absorption (Fig. 6, curves 2 and 3). The spectrum edge of oxygen photoadsorption quantum efficiency is shifted to the long-wave range (550 nm) in comparison with the edge of spectral dependence of CO_2 photodesorption quantum efficiency (500 nm), see Fig. 4.

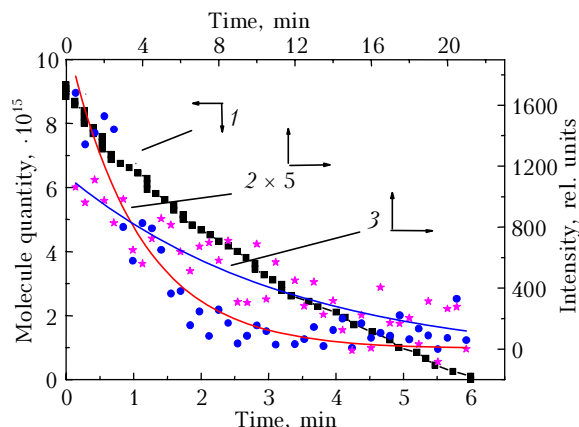


Fig. 5. Kinetics of photoinduced adsorption on TiO_2 : manometric data on oxygen photosorption from dry air (curve 1); data of the 32nd mass intensity variations in the mass-spectrum when oxygen photosorbing from the mixture of dry air with freon 134a (curve 2); reduction of adsorbed CO_2 amount when TiO_2 illuminating through the UVC filter (photodesorption, mass-spectrometric data) (curve 3).

It can be supposed that the oxygen photosorption on the investigated type of titanium dioxide does not result from interaction of oxygen with light-induced electron centers of the surface. Gas-phase oxygen spending due to its photoadsorption results from interaction of oxygen molecules with the compounds, which were adsorbed on the TiO_2 surface from air earlier, i.e., after titanium dioxide producing and holding.

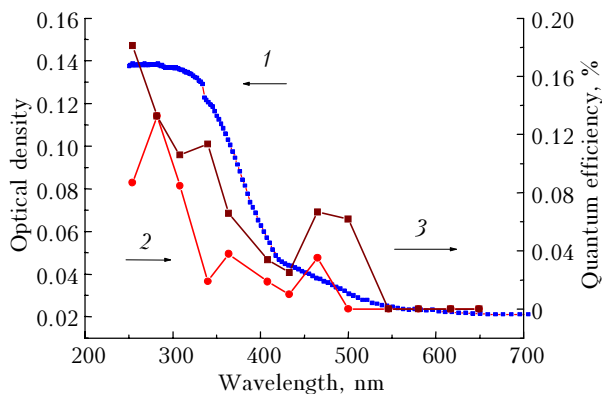


Fig. 6. Spectral dependences for the titanium dioxide produced from combustion of titanium particles in air: SDF of titanium dioxide powder used in the reactor (1); oxygen photosorption from dry air (2); oxygen photosorption from the mixture of dry air with freon 134a (3).

Recorded kinetics of oxygen photosorption is similar to those of the first-order reaction while the kinetics of single gases photoadsorption on metal oxides (photoadsorption on surface centers formed by illumination) after thermo-vacuum treatment of the oxides has a more complicated character.^{17,23,24} Variations of the time constant of CO_2 photodesorption kinetics in the presence of oxygen in the reaction volume and the increase of the carbon

dioxide amount, formed in this case, indicate the interaction of oxygen with sorbate compounds. Gas-phase oxygen spending for light oxidation of organic compounds, adsorbed on TiO_2 , was assumed in Ref. 25.

Conclusions

Thus, titanium dioxide, produced from combustion of a pyrotechnic mixture, containing titanium particles, is similar to titanium dioxide, produced in other ways, in its optical and chemical properties. Widths of band gaps of differently produced TiO_2 are the same; the absorption in the spectrum range up to the self-absorption edge is observed and related to the titanium dioxide stoichiometry disruption.

CO_2 photodesorption and oxygen photoadsorption are observed for TiO_2 in the wide range of troposphere sunlight spectrum. At the same time, we did not observe interactions of titanium dioxide surface with neither methane nor ethane or their halogen derivatives in experiments, but photocatalytic oxidation of carbon dioxide was observed.

It can be supposed that titanium dioxide produced from the combustion of a pyrotechnic mixture in air will be active in the reactions, in which photocatalytic oxidation is observed, according to reference data, e.g., oxidation of ethylene and its halogen derivatives, oxidation of carboxylic acids, spirits, etc.

Acknowledgements

This work was supported by the Program "Leading Russian Scientific Schools" (Grant NSH No. 2526.2006.3).

References

1. B.Z. Eapen, V.K. Hoffmann, M. Schoenitz, and E.L. Dreizin, *Combustion Sci. and Technol.* **176**, No. 7, 1055–1069 (2004).
2. I.E. Molodetsky, E.L. Dreizin, E.P. Vicenzi, and C.K. Law, *Combustion and Flame* **112**, No. 3, 522–532 (1998).
3. Ya.I. Goldshleger and E.Ya. Shafirovich, *Fiz. Goreniya i Vzryva* **35**, No. 1, 42–50 (1999).
4. V.N. Parmon and V.S. Zakharenko, *Cat. Tech.* **5**, No. 2, 96–115 (2001).
5. *Proc. of 2nd European Meeting on Solar-chemistry and Photocatalysis: Environmental Application*, Saint-Avold, France, (2002).
6. V.S. Zakharenko, V.N. Parmon, and K.I. Zamaraev, *Kinet. i Katal.* **38**, No. 1, 140–144 (1997).
7. S.A. Khromova, V.V. Karasev, A.A. Onischuk, O.G. Glotov, and V.E. Zarko, in: *Nonequilibrium Processes*, G. Roy, S. Frolov, A. Starik, eds. (Toros Press, Moscow, 2005), pp. 225–234.
8. V.V. Karasev, S.A. Khromova, A.A. Onischuk, O.G. Glotov, and E.A. Pilugina, in: *Siberian Aerosols* (Publishing House of IAO SB RAS, Tomsk, 2005), p. 5.

9. I. Kostov, *Mineralogy* (Mir, Moscow, 1971), 584 pp.
10. R.I. Bickley, T. Gonzalez-Carreno, J.S. Lees, L. Palmisano, and R.J.D. Tilley, *J. Solid State Chem.* **92**, No. 1, 178–186 (1991).
11. V.S. Zakharenko, *Catal. Today* **39**, No. 3, 243–249 (1997).
12. P. Jackson and G.D. Parfitt, *J. Chem. Soc. Faraday Trans.* **68**, No. 1, 896–906 (1972).
13. L. Kurbon, M. Formenti, F. Juillet, A.A. Lisachenko, J. Martain, and S.J. Teichner, *Kinet. i Katal.* **14**, No. 1, 110–115 (1973).
14. A. Mills and S.J. Le Hunte, *Photochem. and Photobiol., A: Chemistry* **108**, No. 1, 1–35 (1997).
15. V.L. Rapoport, B.M. Antipenko, and M.G. Malkin, *Kinet. i Katal.* **9**, No. 6, 1306–1314 (1968).
16. Yu.P. Solonitsin, G.N. Kuzmin, A.L. Shurygin, and V.M. Yurkin, *Kinet. i Katal.* **17**, No. 5, 1267–1272 (1976).
17. L.L. Basov, O.B. Konova, and G.N. Kuzmin, in: *X-ray and Catalytic Processes in Disperse Media* (Nauka, Novosibirsk, 1992), pp. 78–108.
18. V.S. Zakharenko and V.N. Parmon, *Kinet. i Katal.* **41**, No. 6, 834–838 (2000).
19. N. Djeghri, M. Formenti, F. Juillet, and S.J. Teichner, *Faraday Discussion, Chem. Soc.* **58**, No. 1, 185–193 (1974).
20. V.A. Isidorov, E.M. Klokova, V.G. Povarov, and S. Klokova, *Catal. Today* **39**, No. 3, 233–242 (1997).
21. M.R. Nimies, W.A. Jacoby, D.M. Blake, and T.A. Milne, *Environ. Sci. and Technol.* **27**, No. 3, 732–739 (1993).
22. M.D. Driessen, A.L. Goodman, T.M. Miller, G.A. Zaharias, and V.U. Grassian, *J. Phys. Chem. B* **102**, No. 3, 549–556 (1998).
23. L.L. Basov, V.A. Kotelnikov, A.A. Lisachenko, V.L. Rapoport, and Yu.P. Solonitsin, in: *Photonics Progress* (Publishing House of the Leningrad University, Leningrad, 1969), No. 1, pp. 78–111.
24. Yu.P. Solonitsin, *Kinet. i Katal.* **7**, No. 4, 480–488 (1966).
25. Yu.P. Solonitsin, “*Oxygen photosorption on zinc oxide*,” *Cand. Phys.-Math. Sci. Dissert.*, Leningrad, (1965), 118 pp.